Electronic Supplementary Material (ESI) for Physical Chemistry Chemical Physics.
This journal is © the Owner Societies 2015

SUPPLEMENTAL MATERIAL

Realizing Chemical Codoping in TiO_2

Fang Wang,[a,b] Yi-Yang Sun,[c] John B. Hatch,[b] Hui Xing,[b] Xuechen Zhu,[b] Hongwang Zhang,[b] Xiaohong Xu,[a] Hong Luo,[b] S. Perera,[b] Shengbai Zhang*[c] and Hao Zeng*[b]

[a]*School of Chemistry and Materials Science, Shanxi Normal University, Linfen 041004, China*

[b]*Department of Physics, University at Buffalo SUNY, Buffalo, New York 14260, USA*

[c]*Department of Physics, Applied Physics & Astronomy, Rensselaer Polytechnic Institute, Troy, New York 12180, USA*

*Emails: zhangs9@rpi.edu; haozeng@buffalo.edu

The supplemental material provides both experimental and theoretical details, including SEM, TEM, and XRD patterns and some references.

Part 1: Experimental Details

1. Chemical synthesis

All chemicals were used as received without further purification. Titanium (TTIP) was used as the titanium source. Trioctylphosphine (TOP) and urea were chosen as precursors for the phosphorus and nitrogen doping. Both urea and NH_3 have been used as N sources for TiO_2 doping in earlier studies[1,2]. Urea is chosen in this work due to its ease of handling and its environmental-friendly nature. The choice of P source is another key factor

for the success of the N-P chemical codoping. TOP was used in earlier work as a P source for low-temperature conversion of metals into metal phosphides[3]. It is therefore chosen here, since the similarity of the oxidation state of the P source to the target environment (i.e., P^{3-}) is necessary.

The as-prepared codoped TiO_2 sample with sequential doping of nitrogen followed by phosphorous was labeled as NP-TiO_2, while the one with reverse doping order was labeled as PN-TiO_2. Accordingly, the phosphor or nitrogen monodoped TiO_2 samples were labeled as P-TiO_2 and N-TiO_2, respectively. The first process is the synthesis of pure anatase TiO_2 powder[4]. 0.3 ml TTIP was dissolved in 12 ml anhydrous ethanol. The solution was stirred magnetically for several minutes, and then 1 ml nitric acid was added to adjust the acidity of the solution in order to form the gels slowly. At room temperature 3 ml deionized water was added dropwise to the solution under vigorous stirring. The mixture was hydrolyzed in a water bath at 80 ^{o}C for 24 h to form a white gel precipitate, and then hydrothermally treated in a Teflon-lined autoclave at 175 ℃ for 3 h to obtain the anatase structure of TiO_2[5]. As a result, the powder sample was obtained by drying in air at 60 ^{o}C. N-TiO_2 was obtained by mixing 0.6 g urea with deionized water during hydrolytic synthesis of TiO_2. PN-TiO_2 was synthesized by mixing 0.6 g urea and P-TiO_2 nanoparticles into a high-pressure autoclave with ethanol as a supercritical fluid and heating at 190 ℃ for 5 h. P-TiO_2 and NP-TiO_2 were obtained by mixing TiO_2 or N-TiO_2, respectively with TOP in a flask and heating the mixture to the reflux temperature for 12 h under nitrogen atmosphere. All samples were cleaned by acetone, ethanol and water for three times to remove surface adsorbed contaminants.

2. Scanning tunneling spectroscopy measurements

The scanning tunneling microscopy and scanning tunneling spectroscopy were done in an Omicron UHV/variable temperature scanning probe microscope, at room temperature and a base vacuum of 3×10^{-11} torr. The carefully washed TiO_2 nanoparticles were drop-cast on a gold substrate and dried in N_2. The thickness is carefully controlled to obtain satisfactory conductivity for STS measurement. The *I-V* and *dI/dV* vs. sample bias *V* measurements were done by turning off the feedback mechanism at each pixel and holding the tip-sample distance constant while stepping incrementally through the voltage range in 200 steps. The *I-V* curves were measured simultaneously with the *dI/dV*. We obtained *dI/dV* at each of the 200 DC voltage bias steps by employing a modulation bias technique which requires superimposing a small AC bias over the DC voltage bias during the STS voltage bias sweep. The modulation frequency is 6 kHz and amplitude is 75 mV. The nanocrystals were deposited on gold substrates. The measurement tip is Pt/Ir. The modulation in the tunneling current *dI* is amplified by the STM electronics and turned into a voltage signal. The magnitude of the *dI* signal for each voltage step is extracted by the lock-in amplifier and stored. We collected STS on selected areas of 1μm ×1μm size using 125×125 pixel scan resolution. A threshold of 2.5% of the maximum *dI/dV* value was chosen to cut the *dI*/*dV* curve, and the difference between positive and negative bias was taken to be the band gap. The threshold was chosen so that the most probable band gap of the undoped TiO_2 is 3.0 eV. The threshold *dI/dV* value, the intersection of the positive and negative bias voltages and the band gap determination for each pixel is automated using a home-made C++ program.

Part 2: Theoretical details

Our hybrid functional calculation is based on the mixing of screened Hartree-Fock exchange (as introduced in the HSE scheme) into the conventional PBE exchange using a mixing parameter of 0.18. Such a hybrid scheme gives a band gap for anatase TiO_2 of 3.25 eV and enthalpy of formation of 9.6 eV/TiO_2 formula. Both values are in good agreement with experimental values.

Regarding the electronic structure in Fig. 1(b), for an isolated N_O defect, three defect levels emerge in the band gap of TiO_2, which are mainly contributed by N 2p orbitals. Each of them is spin-polarized giving rise to six spin orbitals, five of which are occupied and located close to the valence band. Only one empty spin-down orbital is located higher in the band gap. This result indicates that the N dopant on O site is weakly involved in the bonding with the neighboring Ti atoms, which is common for N doping in other oxide materials, such as ZnO[6] and SnO_2[7]. The high-lying empty spin orbital is because of the Hartree-Fock component in the hybrid functional, which enhances the spin splitting compared with conventional DFT functionals.

To calculate defect formation energy, we used the standard formalism[8,9]. Taking the case of P-on-O (P_O) as an example, the formation energy $\Delta H(P_O) = E(P_O) - E_0 - \mu_P + \mu_O$, where E_0 is the total energy of the perfect supercell without any defect, $E(P_O)$ is the total energy of the supercell containing a P_O defect, μ_P and μ_O are the chemical potentials of P and O, respectively. μ_P is taken to be the total energy per P atom in red phosphorous. $\mu_O = \mu^0_O + \mu'_O$, where μ^0_O is taken to be total energy per O atom in an isolated O_2 molecule. Similarly, $\mu_{Ti} = \mu^0_{Ti} + \mu'_{Ti}$, where μ^0_{Ti} is taken to be total energy per Ti atom in Ti metal (*hcp* phase). To

maintain a stable TiO_2 phase, it is required that $\mu'_{Ti} + 2\mu'_O = -\Delta H(TiO_2) = -9.6$ eV[8]. Thus, μ'_O can vary between -4.8 eV to 0 eV, where $\mu'_O = 0$ eV corresponds to O-rich condition, while $\mu'_O = -4.8$ eV corresponds to Ti-rich condition.

Our DFT calculation shows that (see Fig. S4) without the presence of N, the formation energy for a P-on-Ti (P_{Ti}) defect is lower than that for a P-on-O (P_O) defect over a wide range of O chemical potential. In the presence of N dopants, however, the formation energy of a P_O defect in the neighborhood of a N_O defect can be lowered by 3.4 eV because of the new chemical bonding. As a result, under the Ti-rich condition, it is possible for a P dopant to occupy an O site.

The calculation of defect transition level, $\varepsilon(q/q')$, follows the method as described in, e.g., Refs. [9,10]. Taking P_{Ti} as an example, its $\varepsilon(0/+)$ level is calculated by

$$\varepsilon(0/+) = E(P_{Ti}^{0}) - E(P_{Ti}^{+}) - E_{VBM},$$

where $E(P_{Ti}^{0})$ and $E(P_{Ti}^{+})$ are the total energy of the supercell containing the P_{Ti} defect in neutral and 1+ charge state, respectively, and E_{VBM} is the energy of valence band maximum of bulk anatase TiO_2. Our calculation shows that P_{Ti} has a $\varepsilon(0/+)$ level between 3.24 to 3.26 eV above the VBM, where the 0.02 eV uncertainty is because of the Madelung correction[10]. Considering the calculated band gap of 3.25 eV, this result suggests that P_{Ti} is a shallow donor and does not introduce any deep electronic levels in the band gap.

Supplemental figures

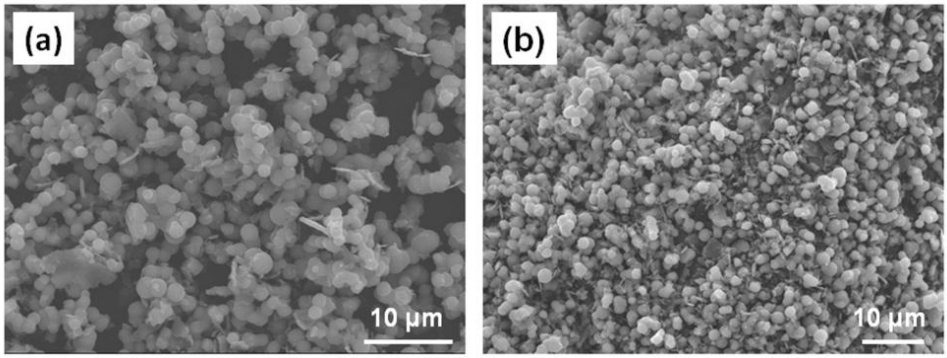

Figure S1, SEM images of (a) N-TiO_2 (N: 2.4%) and (b) NP-TiO_2 (N: 1%, P: 3.7%). Uniform and nearly spherical TiO_2 particles with sizes of about 1 μm were obtained for both N-doped only and NP-doped TiO_2. P doping can hardly affect the morphology of N-TiO_2 although P doping process was carried out under higher temperature after N doping.

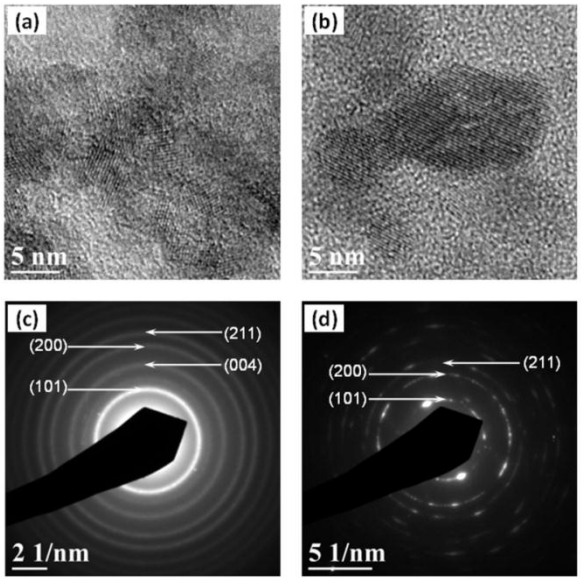

Figure S2, High-resolution TEM images of (a) undoped TiO_2 and (b) NP-TiO_2; (c) and (d) show the corresponding selected area electron diffraction (SAED) patterns. The particles with crystallite sizes ranging from 5 to 10 nm can be found from undoped TiO_2 and NP-TiO_2, indicating that the particles in **Fig. S1** may be some microspheres composed of many smaller TiO_2 particles with a diameter of 5-10 nm. The SAED patterns show that the anatase structure was retained upon doping.

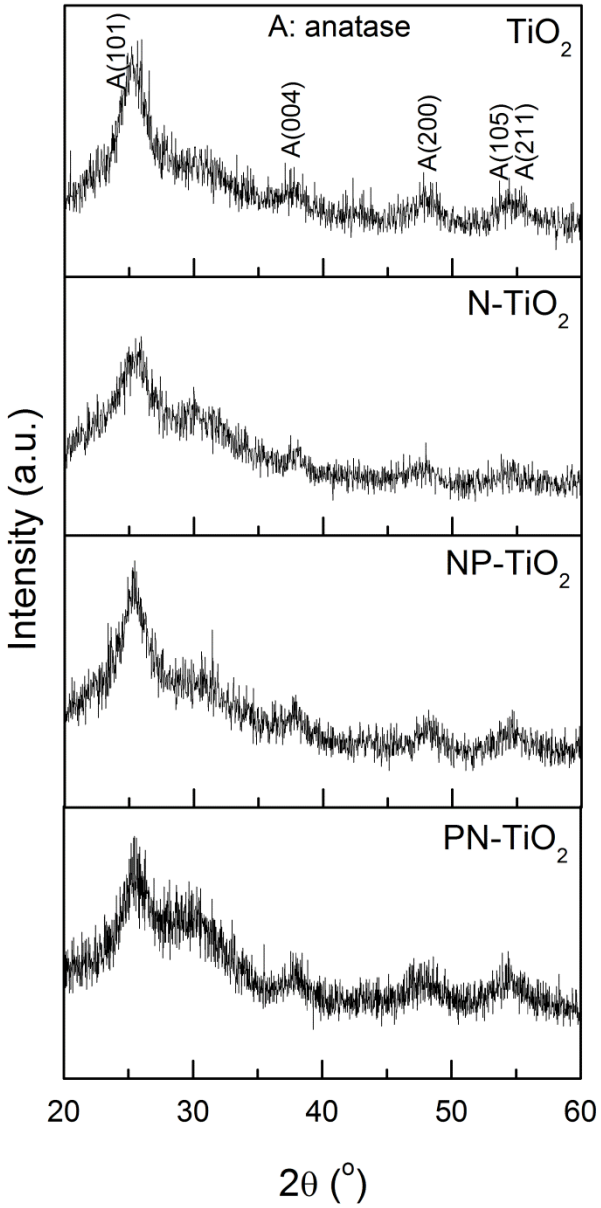

Figure S3, X-ray diffraction patterns of TiO_2, N-TiO_2, NP-TiO_2, and PN-TiO2. All samples demonstrate anatase structure. The large half-peak width and low intensity of (101) diffraction peaks at 2θ of 25^o further confirm the microsphere of doped TiO_2 was composed of small nanoparticles.

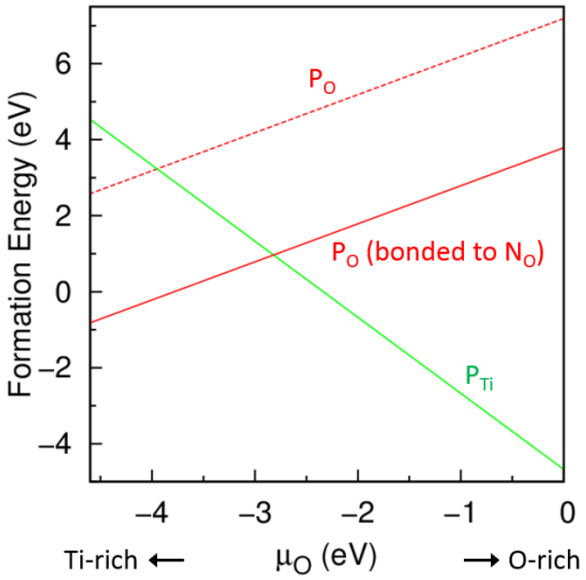

Figure S4, Formation energy of P_{Ti}, P_O and P_O bonded to a N_O defect as a function of oxygen chemical potential.

References

[1] Yuan, J., Chen, M. X., Shi, J. W. & Shangguan, W. F. Preparations and photocatalytic hydrogen evolution of N-doped TiO_2 from urea and titanium tetrachloride. *Int. J. Hydrogen Energ.* **31,** 1326-1331 (2006).

[2] Guo, W., Shen, Y. H., Boschloo, G., Hagfeldt, A. & Ma, T. L. Influence of nitrogen dopants on N-doped TiO_2 electrodes and their applications in dye-sensitized solar cells. *Electrochim. Acta* **56,** 4611-4617 (2011).

[3] Henkes, A. E. & Schaak, R. E. Trioctylphosphine: a general phosphorus source for thelow-temperature conversion of metals into metal phosphides. *Chem. Mater.* **19,** 4234-4242 (2007).

[4] Bischoff, B. L. & Anderson, M. A. Peptization process in the sol-gel preparation of porous anatase (TiO_2). *Chem. Mater.* **7,** 1772-1778 (1995).

[5] Chae, S. Y., Park, M. K., Lee, S. K., Kim, T. Y., Kim, S. K. & Lee, W. I. Preparation of size-controlled TiO_2 nanoparticles and derivation of optically transparent photocatalytic films. *Chem. Mater.* **15,** 3326-3331 (2003).

[6] Lyons, J. L., Janotti, A. & Van de Walle, C. G. Why nitrogen cannot lead to p-type conductivity in ZnO. *Appl. Phys. Lett.* **95,** 252105 (2009).

[7] Scanlon, D. O. & Watson, G. W. On the possibility of p-type SnO_2. *J. Mater. Chem.* **22,** 25236 (2012).

[8] Zhang, S. B. & Northrup, J. E. Chemical potential dependence of defect formation energies in GaAs: Application to Ga self-diffusion. *Phys. Rev. Lett.* **67,** 2339 (1991).

[9] Van de Walle, C. G. & Neugebauer, J. First-principles calculations for defects and impurities: Applications to III-nitrides. *J. Appl. Phys.* **95,** 3851 (2004).

[10] Zhang, S. B. The microscopic origin of the doping limits in semiconductors and wide-gap materials and recent developments in overcoming these limits: a review. *J. Phys.: Condens. Matter*. **14,** R881 (2002).